

Dephasing in the adiabatic rapid passage in quantum dots: the role of phonon-assisted biexciton generation

Krzysztof Gawarecki,¹ Sebastian Lüker,² Doris E. Reiter,² Tilmann Kuhn,² Martin Gläsel,³ Vollrath Martin Axt,³ Anna Grodecka-Grad,⁴ and Paweł Machnikowski^{1,*}

¹*Institute of Physics, Wrocław University of Technology, 50-370 Wrocław, Poland*

²*Institut für Festkörpertheorie, Universität Münster, 48149 Münster, Germany*

³*Institut für Theoretische Physik III, Universität Bayreuth, 95440 Bayreuth, Germany*

⁴*QUANTOP, Danish National Research Foundation Center for Quantum Optics, Niels Bohr Institute, University of Copenhagen, DK-2100 Copenhagen Ø, Denmark*

We study the evolution of an exciton confined in a quantum dot adiabatically controlled by a frequency-swept (chirped) laser pulse in the presence of carrier-phonon coupling. We focus on the dynamics induced by a linearly polarized beam and analyze the decoherence due to phonon-assisted biexciton generation. We show that if the biexciton state is shifted down by a few meV, as is typically the case, the resulting decoherence is strong even at low temperatures. As a result, efficient state preparation is restricted to a small parameter area corresponding to low temperatures, positive chirps and moderate pulse areas.

PACS numbers: 78.67.Hc, 71.38.-k, 42.50.Ct, 03.65.Yz

I. INTRODUCTION

The recently demonstrated^{1,2} high-fidelity preparation of a single exciton state in a self-assembled quantum dot (QD) by means of adiabatic evolution induced by a chirped laser pulse (referred to as *adiabatic rapid passage*, ARP) opens new possibilities of charge control in QDs. In contrast to the more traditional Rabi flops³ as well as to methods based on voltage control^{4,5}, ARP is much less sensitive to the details of the driving field. In particular, in the ideal case, the ARP technique ensures the full inversion of occupation between the empty dot and exciton states as soon as the pulse intensity reaches the threshold for the adiabatic passage. ARP can also be used to generate entanglement in double dot systems⁶.

However, as QDs are embedded in a semiconductor crystal matrix, carrier-phonon interactions are usually found to considerably limit the fidelity of various optical control schemes. Phonon-induced decoherence processes are inevitable in such systems and lead to loss of information. These mechanisms have been investigated theoretically⁷⁻¹⁴ and have been confirmed experimentally¹⁵⁻¹⁷. As recently shown¹⁸⁻²⁰, in the case of the ARP the role of phonon coupling in the state preparation is essential. As the adiabatic evolution follows one of the spectral branches corresponding to dressed exciton states, the carrier phonon coupling leads to transitions to the other branch. Depending on whether the upper or lower branch is followed (which, in turn, depends on the direction of the chirp), the transition is assisted by phonon emission or absorption, respectively. As a consequence, at low temperatures the phonon-induced decoherence leads to a strong asymmetry in the final occupation of the exciton state depending on the sign of the chirp¹⁸. While the analysis performed in Ref. 18 was based on a two-level model, corresponding to the excitation with a circularly polarized laser pulse, in actual ex-

periments linearly polarized beams have been used. This choice is, on the one hand, motivated by practical aspects of the experiment: If optical detection schemes are employed then, in view of the need to excite and detect in the same frequency range, using linearly cross-polarized light for excitation and detection reduces the amount of stray light incident on the detector¹. On the other hand, in QDs with a large fine structure splitting and for strong chirps (which enhance the actual pulse duration), it may be favorable to address the fine structure eigenstates instead of the angular momentum eigenstates, which amounts to using linear polarization of light. In this case, however, the selection rules allow the coupling to the biexciton state and phonon-assisted biexciton generation²¹ may occur even at low temperatures, as the biexciton state is typically shifted to lower energies.

In this paper, we study the evolution of the exciton-biexciton system driven by a linearly polarized chirped pulse in the regime of the ARP in the presence of the coupling to acoustic phonons. We show that including the biexciton state, which becomes relevant for linearly polarized laser pulses¹, indeed opens a new decoherence path related to phonon-assisted transitions to the biexciton state. As a result, the fidelity of exciton state preparation drops down considerably in particular in most of the parameter areas where almost ideal evolution was predicted by the two-level model. Thus, high-fidelity control becomes restricted to the range of moderate pulse areas for positive chirps and at low temperatures only, unless circular polarized pulses are used to suppress biexcitonic excitations.

The paper is organized as follows. In Sec. II, we describe the system and define the model used in our study. Sec. III introduces our method of simulation of the open system dynamics. The results are presented in Sec. IV. Finally, Sec. V concludes the paper.

II. MODEL

The biexciton system in the QD, restricted to the lowest bright states, is modeled as a four-level system with $|0\rangle$ representing the empty dot, $|X\rangle, |Y\rangle$ being the two exciton states with different linear polarizations and $|B\rangle$ denoting the biexciton state. The corresponding Hamiltonian is

$$H_X = E_X|X\rangle\langle X| + E_Y|Y\rangle\langle Y| + \tilde{E}_B|B\rangle\langle B|,$$

where E_X, E_Y and \tilde{E}_B are the energies of the two exciton polarization eigenstates (with a possible energy difference resulting from the fine structure splitting) and of the biexciton state, respectively.

The system is driven by a X -linearly polarized chirped Gaussian pulse with the original envelope

$$\Omega_0(t) = \frac{\Theta}{\sqrt{2\pi}\tau_0} \exp\left(-\frac{t^2}{2\tau_0^2}\right),$$

where Θ is the original pulse area (before chirping) and τ_0 is the initial duration (pulse length). The central frequency ω_0 is chosen in resonance with the transition to the single exciton state $|X\rangle$. We assume that the linear chirp is obtained by passing this pulse through a Gaussian chirp filter²² with the chirp coefficient α . This results in the chirped pulse envelope

$$\Omega(t) = \frac{\Theta}{\sqrt{2\pi}\tau_0\tau} \exp\left(-\frac{t^2}{2\tau^2}\right),$$

with the chirped pulse length $\tau = (\alpha^2/\tau_0^2 + \tau_0^2)^{1/2}$, and the frequency chirp rate $a = \alpha/(\alpha^2 + \tau_0^4)$. The Hamiltonian describing the coupling to the chirped pulse in the rotating wave approximation is

$$H_{\text{las}} = \frac{\hbar\Omega(t)}{2} (|0\rangle\langle X| + |X\rangle\langle B|) e^{i\omega_0 t + iat^2/2} + \text{h.c.}$$

Thus, for X -linear polarization, the coupling is $|0\rangle \leftrightarrow |X\rangle \leftrightarrow |B\rangle$ and the other single-exciton state $|Y\rangle$ is decoupled (it is not coupled by phonon transitions, either²³). Therefore, only a three-level model is needed²⁴.

The idea of the adiabatic passage²⁵ is to drive the system state adiabatically along one of the spectral branches corresponding to the instantaneous eigenstates of the Hamiltonian $H_0 = H_X + H_{\text{las}}$. These instantaneous eigenstates are shown in Fig. 1 for the biexciton shift $E_B = \tilde{E}_B - 2E_X = -2.0$ meV and $\hbar\omega_0 = E_X$. The branch followed by the system state is plotted with a thicker line. In Fig. 1(a), we assume a positive chirp ($\alpha > 0$), while in Fig. 1(b) a negative chirp is assumed. For pulse intensities above the ARP threshold, the central anticrossing at $t = 0$ (between the vacuum and exciton states) is passed adiabatically along a single spectral branch. On the contrary, the two other anticrossings away from $t = 0$ (exciton-biexciton and vacuum-biexciton) are met when the pulse is very weak, hence they are very narrow (in the

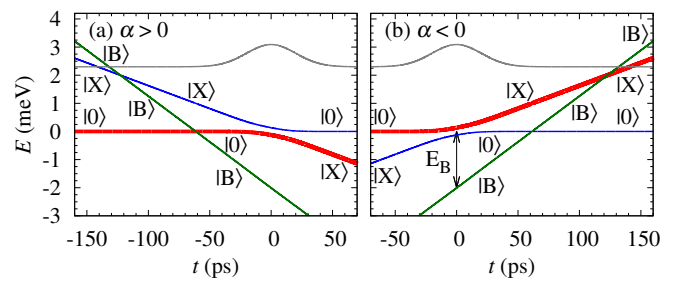


FIG. 1: (Color online) The adiabatic spectral branches of the optically driven QD system for $\Theta = 2\pi$, $\tau_0 = 2$ ps, $|\alpha| = 40$ ps² and $E_B = -2$ meV: (a) positive chirp; (b) negative chirp. The evolution starting from the ground state follows the thick red line. The gray solid line represents the pulse envelope $\Omega(t)$ which has been shifted upwards for clarity.

case shown here, the widths of both of these anticrossings are below 10 μeV , unresolved in Fig. 1). At such narrow anticrossings, the sweep rate is very high compared to the distance between the two levels, which leads to a nearly purely non-adiabatic evolution: these anticrossings are almost completely crossed by the evolving system state, that is, the system nearly completely jumps to the other branch. As a result, the charge configuration does not change here, as opposed to the central anticrossing. This qualitatively different system evolution is reflected by the color coding of the lines in Fig. 1. At narrow anticrossings, which are traversed by the system evolution, the single line color and width is kept across the resonance. On the contrary, at broad anticrossings, lines of a given color and width follow a single branch. In this way, in our color coding, the actual system evolution (under the driving conditions as discussed here) corresponds to following always the red (thick) line in Fig. 1.

For the parameter range corresponding to the experiments^{1,2} excitation of optical phonon modes is excluded by the spectral properties of the system. In consequence, the coupling to acoustic phonons can be expected to dominate as a source of decoherence. The carrier-phonon interaction is described in terms of the usual independent boson Hamiltonian, $H_{\text{int}} = S \otimes R$, with

$$S = |X\rangle\langle X| + |Y\rangle\langle Y| + 2|B\rangle\langle B|$$

and

$$R = \sum_{\mathbf{k}} g_{\mathbf{k}} b_{\mathbf{k}} + \text{h.c.},$$

where $b_{\mathbf{k}}$ are phonon annihilation operators. We assume that the biexcitonic and excitonic wave functions can be factorized into products of single particle wave functions which are the same for both exciton and biexciton. This is well justified in the strong confinement limit where the wave functions are mostly determined by the confinement potentials. The coupling constants, accounting for the

deformation potential interaction, can then be written as

$$g_{\mathbf{k}} = \sqrt{\frac{\hbar k}{2\rho v c}} [D_e \mathcal{F}_e(\mathbf{k}) - D_h \mathcal{F}_h(\mathbf{k})],$$

where v is the normalization volume, ρ is the crystal density, c is the speed of sound, $D_{e(h)}$ is the deformation potential constant for an electron (hole) and

$$\mathcal{F}_{e(h)}(\mathbf{k}) = \int d^3r |\psi_{e(h)}(\mathbf{r})|^2 e^{i\mathbf{k}\cdot\mathbf{r}}$$

are the form factors for the electron (hole) wave functions $\psi_{e(h)}(\mathbf{r})$. Finally, the phonon reservoir is described by the Hamiltonian

$$H_{\text{ph}} = \sum_{\mathbf{k}} \hbar\omega_{\mathbf{k}} b_{\mathbf{k}}^\dagger b_{\mathbf{k}},$$

where $\omega_{\mathbf{k}} = ck$ are the phonon frequencies.

The system is conveniently described in the non-uniformly rotating frame defined by the unitary transformation $e^{iA(t)}$, where

$$A(t) = \left(\frac{E_X}{\hbar} t + \frac{1}{2} at^2 \right) (|X\rangle\langle X| + 2|B\rangle\langle B|) + \frac{E_Y}{\hbar} t |Y\rangle\langle Y|.$$

We assume that the central frequency of the pulse is tuned to the transition to the X state, that is, $\hbar\omega_0 = E_X$. The resulting Hamiltonian is $H = H'_X + H'_{\text{las}} + H_{\text{int}} + H_{\text{ph}}$, with

$$\begin{aligned} H'_X &= e^{iA(t)} H_X e^{-iA(t)} - \hbar\dot{A}(t) \\ &= \hbar\Delta(t) |X\rangle\langle X| + (2\hbar\Delta(t) + E_B) |B\rangle\langle B|, \end{aligned}$$

where $\Delta(t) = -at$, and

$$\begin{aligned} H'_{\text{las}} &= e^{iA(t)} H_{\text{las}} e^{-iA(t)} \\ &= \frac{\hbar\Omega(t)}{2} (|0\rangle\langle X| + |X\rangle\langle B|) + \text{h.c.} \end{aligned}$$

III. METHOD OF SIMULATION

To simplify the numerical simulation, we perform the unitary transformation defined by the operator

$$\mathbb{W} = |0\rangle\langle 0| + (|X\rangle\langle X| + |Y\rangle\langle Y|) W + |B\rangle\langle B| W^2,$$

where

$$W = \exp \left[\sum_{\mathbf{k}} \frac{g_{\mathbf{k}}}{\omega_{\mathbf{k}}} (b_{\mathbf{k}} - b_{-\mathbf{k}}^\dagger) \right]. \quad (1)$$

Upon this transformation and expanding to the leading order in the coupling constants, the Hamiltonian may be written as

$$\tilde{H} = \mathbb{W} H \mathbb{W}^\dagger = H_1 + H_{\text{ph}} + V,$$

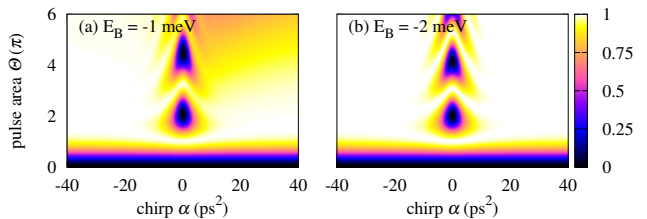


FIG. 2: (Color online) The final occupation of the single-exciton state (color coded) as a function of the original pulse area Θ and the chirp α in the absence of coupling to phonons: (a) for $E_B = -1.0$ meV (b) for $E_B = -2.0$ meV.

where $H_1 = H'_X + wH'_{\text{las}}$ and

$$V = \frac{\hbar\Omega(t)w}{2} (|0\rangle\langle X| + |X\rangle\langle B|) (W^\dagger - \langle W^\dagger \rangle) + \text{h.c.}$$

Here

$$w = 1 - \frac{1}{2} \sum_{\mathbf{k}} \left| \frac{g_{\mathbf{k}}}{\omega_{\mathbf{k}}} \right|^2$$

accounts for the phonon-induced renormalization of the pulse amplitude in the slow driving limit^{9,16}. We assume that the central frequency of the driving pulse is corrected for the phonon-induced energy shifts.

The evolution of the reduced density matrix of the charge subsystem is then found by numerically solving the lowest-order time-convolutionless (TCL) evolution equation^{26,27}

$$\dot{\rho}(t) = - \int_0^t d\tau \text{Tr}_{\text{ph}} [V(t), [V(\tau), \rho(t) \otimes \rho_{\text{ph}}]],$$

where $V(t)$ is the interaction Hamiltonian V in the interaction picture with respect to $H_1 + H_{\text{ph}}$, ρ_{ph} is the phonon density matrix at the thermal equilibrium, and Tr_{ph} denotes the partial trace with respect to phonon states. While it may be possible to keep the full polaronic transformation [Eq. (1)] throughout the simulations or even to adapt it variationally to a given evolution¹³ and, in this way, to achieve in principle an improved accuracy of the results, our choice to keep only the leading terms is consistent with the lowest order approximation of the TCL generator. More importantly, we have verified that this procedure yields very accurate results under the driving conditions considered here, at least at low and moderate temperatures²⁸.

IV. RESULTS

With the simulation method outlined in Sec. III, we study the exciton dynamics focusing on the possibility of phonon-assisted transitions to the biexciton state, when the system is excited with a linearly polarized laser pulse.

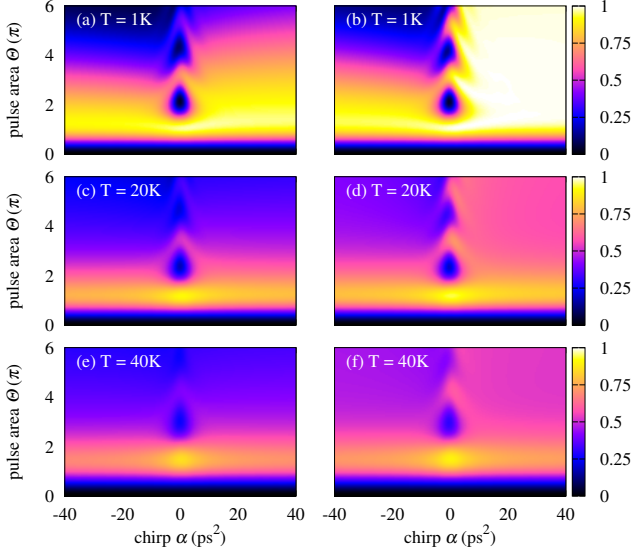


FIG. 3: (Color online) The final occupation of the single-exciton state (color coded) as a function of the original pulse area Θ and the chirp α with phonon effects included: (a,c,e) for $E_B = -2.0$ meV (b,d,f) for $E_B = -8.0$ meV.

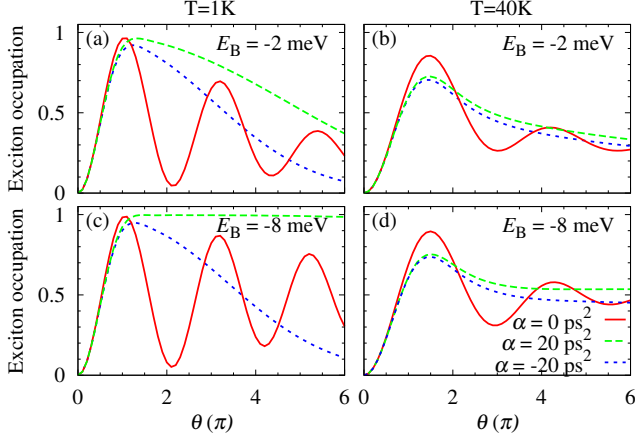


FIG. 4: (Color online) The final occupation of the single-exciton state as a function of the original pulse area Θ at two different temperatures: (a,b) for $E_B = -2.0$ meV; (c,d) for $E_B = -8.0$ meV. The blue dotted line shows the results with chirp $\alpha = -20$ ps², the red solid line represents $\alpha = 0$, while the green dashed line corresponds to $\alpha = 20$ ps².

In our simulations, we assume $\rho = 5360$ kg/m³, $c = 5110$ m/s, $D_e = 7$ eV and $D_h = -3.5$ eV. The electron wave functions are assumed to be Gaussians with the extension $l_e = 4.5$ nm in the xy plane and $l_{e,z} = 1$ nm along the growth direction. In the case of holes, we take $l_h = 0.87l_e$ and $l_{h,z} = 0.87l_{e,z}$ respectively. The pulse length (before chirping) is taken to be $\tau_0 = 2$ ps.

First, we need to assess the degree of perturbation to

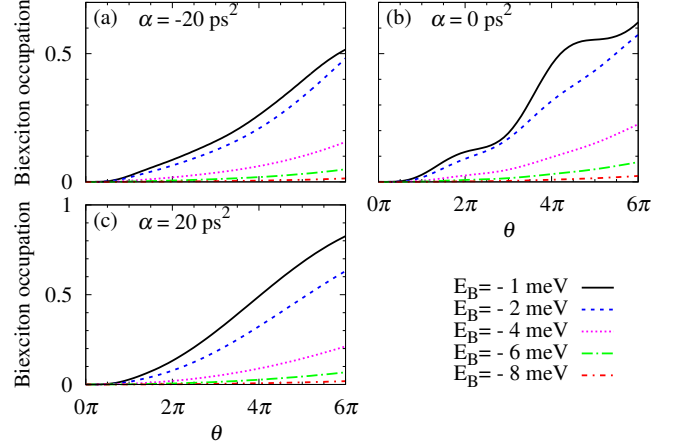


FIG. 5: (Color online) The final biexciton occupation as a function of the original pulse area for different binding energies E_B at $T = 1$ K at three different chirp values: (a) $\alpha = -20$ ps², (b) $\alpha = 0$ ps² and (c) $\alpha = 20$ ps².

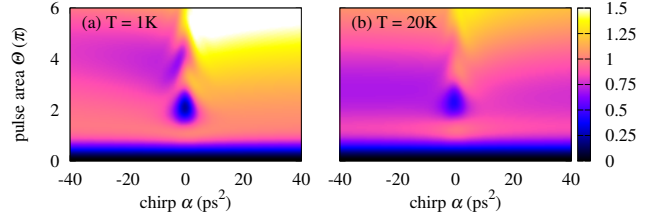


FIG. 6: (Color online) The total number of excitons (color coded) as a function of the original pulse area Θ and the chirp α for $E_B = -2.0$ meV (a) at $T = 1$ K and (b) at $T = 20$ K.

the adiabatic evolution which stems from the additional level crossings with the biexciton (see Fig. 1) and is not related to phonons. To this end, in Fig. 2 we show the single-exciton occupation without carrier-phonon coupling for $E_B = -1.0$ meV and $E_B = -2.0$ meV. The results show a reduction of the final occupation of the single exciton state at higher pulse areas for a very small biexciton shift ($E_B = -1.0$ meV) and positive chirps. We have found that under these conditions, a biexciton occupation on the order of 0.1 occurs (not shown). On the other hand, for the still small value of $E_B = -2.0$ meV, the evolution is nearly unperturbed by the presence of the biexciton state. Thus we conclude that for $|E_B| \gtrsim 2$ meV no direct population of the biexciton occurs with the pulses studied here, as the driving of the exciton to biexciton transition is too off-resonant.

In the next step, we include phonons and consider two cases: a) the biexciton state is shifted by a typical energy ($E_B = -2.0$ meV) below the single-exciton state, b) for comparison, the biexciton is shifted by a very large (and rarely realized) energy ($E_B = -8.0$ meV). In the first case, one expects that phonon-induced transitions to the

biexciton state are efficient. In the second case, due to the large energy separation between the states (beyond the cut-off frequency of the carrier-phonon coupling), the biexciton generation is expected to be negligible and the system can effectively be treated as a two-level system. The simulated evolution of the single exciton occupation for both cases is shown in Fig. 3. The left panels (Fig. 3(a,c,e)) contain results for $E_B = -2.0$ meV, and the right panels (Fig. 3(b,d,f)) for $E_B = -8.0$ meV. The final occupation is calculated as a function of the pulse area Θ and the chirp rate α at three temperatures ($T = 1, 20,$ and 40 K).

Let us start the discussion for the case of the large biexciton shift $E_B = -8.0$ meV and low temperature $T = 1$ K shown in Fig. 3(b). As expected, the results from the two-level model¹⁸ are retrieved and a strong asymmetry in the final occupation with respect to the chirp is seen. In the two-level model, for negative chirp the evolution follows the upper branch and phonon emission leads to damping, while for positive chirps the lower branch is followed and since phonon absorption is almost absent at 1 K a full exciton occupation is reached. In contrast, in Fig. 3(a), for the small biexciton shift $E_B = -2.0$ meV, the influence of the biexciton state can be clearly seen. In particular, for positive chirps a decoherence at high pulse areas is visible due to the opening of the new decoherence channel consisting in transitions to the biexciton state (phonon-assisted biexciton generation). As can be seen in Fig. 1, for a negative biexciton shift (positive biexciton binding energy), this process corresponds to phonon emission no matter which adiabatic branch is followed, hence it is effective irrespective of the sign of the chirp even at low temperatures. Also for negative chirps the damping has become more effective. Thus, only for moderate pulse areas around $\Theta = 2\pi$ a high-fidelity preparation of the single exciton state is possible.

When considering higher temperatures, as seen in Fig. 3(c-f), phonon absorption becomes more likely and now also for positive chirps decoherence due to transitions between the main branches is stronger. Hence, considerable phonon-induced perturbation is seen even in the case of a strongly detuned biexciton (Fig. 3(d,f)). In consequence, the additional effect of the biexciton shift is relatively weak.

For a quantitative analysis we show the final occupation of the single exciton state as a function of pulse area for different chirps $\alpha = -20, 0,$ and 20 ps² in Fig. 4 for $E_B = -2.0$ meV (Fig. 4(a,b)) and for $E_B = -8.0$ meV (Fig. 4(c,d)). The most remarkable difference for the two biexciton shifts is again seen for the positive chirp $\alpha = 20$ ps² at $T = 1$ K (green dashed line). While in Fig. 4(a), for the small biexciton shift, a strong damping of the exciton occupation is found, in Fig. 4(c), for the large biexciton shift, an exciton occupation of one is reached for all pulse areas above the adiabatic threshold. Also the decoherence for the negative chirp $\alpha = -20$ ps² and damping of the Rabi oscillations at zero chirp are stronger in Fig. 4(a) due to the phonon-assisted biexci-

ton generation. At a higher temperature of $T = 40$ K, Fig. 4(b,d), the difference between small and large biexciton shift is less pronounced.

To confirm this interpretation and to analyze more quantitatively the influence of the biexciton shift on the occupations, we performed the simulations for several values of E_B . We varied E_B from -1 meV to -8 meV. The resulting biexciton occupations at $T = 1$ K as a function of the pulse area for three different chirp values are shown in Fig. 5. We find that for each chirp value the biexciton occupation increases with increasing pulse area. This increase, however is most pronounced for small binding energies where occupations larger than 50 % are reached. For the highest binding energy of $E_B = -8.0$ meV even at the highest pulse area used here the occupation remains below 0.03. We have checked that also at $T = 40$ K the occupation of the biexciton state for $E_B = -8.0$ meV is low and thus the system indeed can be treated as a two-level system.

Since in some experiments² a photocurrent detection scheme is used, in which the detection signal is proportional to the total number of photocreated excitons, we have calculated also the total number of excitons in the system, $N_{\text{total}} = N_X + 2N_B$, where N_X and N_B are the occupations of the single- and biexciton state respectively. The results are shown in Fig. 6 for $E_B = -2$ meV at $T = 1$ K (Fig. 6(a)) and $T = 20$ K (Fig. 6(b)). One can see that at a certain level of phonon-assisted biexciton generation the result exceeds 1, which has no sense if interpreted in terms of the two-level model. Moreover, it is clear that even below this limit, the biexciton contribution leads to an overestimated occupation of the single exciton state.

V. CONCLUSIONS

In summary, we have studied the open system evolution of a QD adiabatically controlled by a chirped linearly polarized laser pulse. We have shown that the presence of a biexciton state, which becomes optically coupled for linearly polarized laser pulses¹, opens new decoherence paths related to phonon-assisted biexciton generation. If the biexciton state is shifted down by 1 or 2 meV it becomes accessible via phonon emission processes and the resulting decoherence is strong even at low temperatures. This reduces the achieved occupation of the single exciton state in the parameter range where the chirped pulse control was very efficient in a model without the biexciton state. Since the phonon-assisted biexciton generation increases with the pulse area moderate pulse areas are optimal for the state preparation. On the other hand, if the biexciton shift is larger, the two-level evolution is essentially recovered.

Acknowledgments

This work was supported in part by a Research Group Linkage Project of the Alexander von Humboldt Founda-

tion and by the TEAM programme of the Foundation for Polish Science, co-financed from the European Regional Development Fund. K.G. acknowledges support from the German Academic Exchange Service (DAAD).

-
- * Electronic address: Pawel.Machnikowski@pwr.wroc.pl
- ¹ C.-M. Simon, T. Belhadj, B. Chatel, T. Amand, P. Renucci, A. Lemaitre, O. Krebs, P. A. Dalgarno, R. J. Warburton, X. Marie, and B. Urbaszek, *Phys. Rev. Lett.* **106**, 166801 (2011).
 - ² Y. Wu, I. Piper, M. Ediger, P. Brereton, E. Schmidgall, P. Eastham, M. Hugues, M. Hopkinson, and R. Phillips, *Phys. Rev. Lett.* **106**, 067401 (2011).
 - ³ A. Zrenner, E. Beham, S. Stuffer, F. Findeis, M. Bichler, and G. Abstreiter, *Nature* **418**, 612 (2002).
 - ⁴ S. Stuffer, P. Ester, A. Zrenner, and M. Bichler, *Phys. Rev. Lett.* **96**, 037402 (2006).
 - ⁵ S. Michaelis De Vasconcellos, S. Gordon, M. Bichler, T. Meier, and A. Zrenner, *Nature Photonics* **4**, 545 (2010).
 - ⁶ C. Creatore, R. T. Brierley, R. T. Phillips, P. B. Littlewood, and P. R. Eastham, *Phys. Rev. B* **86**, 155442 (2012).
 - ⁷ J. Förstner, C. Weber, J. Danckwerts, and A. Knorr, *Phys. Rev. Lett.* **91**, 127401 (2003).
 - ⁸ E. A. Muljarov and R. Zimmermann, *Phys. Rev. Lett.* **93**, 237401 (2004).
 - ⁹ A. Krügel, V. M. Axt, T. Kuhn, P. Machnikowski, and A. Vagov, *Appl. Phys. B* **81**, 897 (2005).
 - ¹⁰ P. Kaer, T. R. Nielsen, P. Lodahl, A.-P. Jauho, and J. Mørk, *Phys. Rev. Lett.* **104**, 157401 (2010).
 - ¹¹ M. Glässl, A. Vagov, S. Lüker, D. E. Reiter, M. D. Croitoru, P. Machnikowski, V. M. Axt, and T. Kuhn, *Phys. Rev. B* **84**, 195311 (2011).
 - ¹² D. P. S. McCutcheon and A. Nazir, *New J. Phys.* **12**, 113042 (2010).
 - ¹³ D. P. S. McCutcheon, N. S. Dattani, E. M. Gauger, B. W. Lovett, and A. Nazir, *Phys. Rev. B* **84**, 081305 (2011).
 - ¹⁴ C. Roy and S. Hughes, *Phys. Rev. Lett.* **106**, 247403 (2011).
 - ¹⁵ A. J. Ramsay, A. V. Gopal, E. M. Gauger, A. Nazir, B. W. Lovett, A. M. Fox, and M. S. Skolnick, *Phys. Rev. Lett.* **104**, 017402 (2010).
 - ¹⁶ A. J. Ramsay, T. M. Godden, S. J. Boyle, E. M. Gauger, A. Nazir, B. W. Lovett, A. M. Fox, and M. S. Skolnick, *Phys. Rev. Lett.* **105**, 177402 (2010).
 - ¹⁷ A. Vagov, V. M. Axt, T. Kuhn, W. Langbein, P. Borri, and U. Woggon, *Phys. Rev. B* **70**, 201305 (2004).
 - ¹⁸ S. Lüker, K. Gawarecki, D. E. Reiter, A. Grodecka-Grad, V. M. Axt, P. Machnikowski, and T. Kuhn, *Phys. Rev. B* **85**, 121302(R) (2012).
 - ¹⁹ A. Debnath, C. Meier, B. Chatel, and T. Amand, *Phys. Rev. B* **86**, 161304 (2012).
 - ²⁰ P. R. Eastham, A. O. Spracklen, and J. Keeling, arXiv:1208.5001 (2012).
 - ²¹ F. Findeis, A. Zrenner, G. Böhm, and G. Abstreiter, *Phys. Rev. B* **61**, R10579 (2000).
 - ²² B. Saleh and M. Teich, *Fundamentals of photonics, Wiley series in pure and applied optics* (Wiley-Interscience, New York, 2007).
 - ²³ M. Glässl, M. D. Croitoru, A. Vagov, V. M. Axt, and T. Kuhn, *Phys. Rev. B* **85**, 195306 (2012).
 - ²⁴ E. R. Schmidgall, P. R. Eastham, and R. T. Phillips, *Phys. Rev. B* **81**, 195306 (2010).
 - ²⁵ L. Allen and J. H. Eberly, *Optical resonance and two-level atoms* (Wiley, New York, 1975).
 - ²⁶ H.-P. Breuer and F. Petruccione, *The Theory of Open Quantum Systems* (Oxford University Press, Oxford, 2002).
 - ²⁷ P. Machnikowski, *Phys. Rev. B* **78**, 195320 (2008).
 - ²⁸ K. Gawarecki, S. Lüker, D. E. Reiter, T. Kuhn, M. Glässl, V. M. Axt, A. Grodecka-Grad, and P. Machnikowski, arXiv:1210.6096 (2012).